Synthesis of Size-Controlled Faceted Pentagonal Silver Nanorods with Tunable Plasmonic Properties and Self-Assembly of These Nanorods

Brendan Pietrobon, Matthew McEachran, and Vladimir Kitaev*

Chemistry Department, Wilfrid Laurier University, 75 University Avenue W, Waterloo, Ontario, Canada N2L 3C5

ABSTRACT Monodisperse size-controlled faceted pentagonal silver nanorods were synthesized by thermal regrowth of decahedral silver nanoparticle (AgNPs) in aqueous solution at 95 °C, using citrate as a reducing agent. The width of the silver nanorods was determined by the size of the starting decahedral particle, while the length was varied from 50 nm to 2 μm by the amount of new silver added to the growth solution. Controlled regrowth allowed us to produce monodisperse AgNPs with a shape of elongated pentagonal dipyramid (regular Johnson solid, J_{16}). Faceted pentagonal particles exhibited remarkable optical properties with sharp plasmon resonances precisely tunable across visible and NIR. Due to the narrow size distribution, faceted pentagonal silver nanorods readily self-assembled into the 3-D arrays similar to smectic mesophases. Hexagonal arrangement in the array completely overrode five-fold symmetry of the nanorods. Overall, our findings highlight the importance of pentagonal symmetry in metal nanoparticles and offer a facile method of the preparation of monodisperse AgNPs with controlled dimensions and plasmonic properties that are promising for optical applications and functional self-assembly.

KEYWORDS: silver nanoparticle synthesis · faceted pentagonal rods · monodisperse · size- and length-controlled nanoparticles · tunable plasmonic absorption · rod self-assembly

Shape- and size-controlled metal nanoparticles (MNPs)[1−3] have demonstrated their utility in diverse applications ranging from catalysis[4] to plasmonics[5,6] and optical sensing.[7,8] For such applications, faceted anisotropic MNPs hold several key advantages: a well-defined surface type,[2,4] easy maneuvering of plasmon resonance,[9] and strong electric field enhancement at regular tips and asperities.[10] Surface-enhanced Raman scattering (SERS) benefits greatly from an increase in the magnitude of electric field due to a strong power dependence.[11] Silver nanoparticles are superior to any other metal NPs for SERS; for instance, the second best metal, gold, shows 2 orders of magnitude less enhancement.[12] As a result, significant research efforts have been invested into shape selection and control of AgNPs. In addition to single-crystalline cubes[13] and octahedra,[14] diverse silver nanoshapes, including pentagonal wires,[15] right bipyramids,[16] pentagonal bipyramids,[17] nanobars, and nanorice,[18] were reported based on judicious synthetic stabilization of lattice twinning defects. Pentagonal silver nanowires were one of the earliest twinned silver nanostructures reported[15] and are currently an established area of research in AgNPs.[19] Since pentagonal rods and wires feature pentagonal multiple twinning (PMT),[20,21] decahedra (the simplest shape with PMT[22]) have been proposed but have not been proved explicitly as intermediates to rods and wires.[23] At the same time, there has been only limited progress in achieving control over the length and width of silver nanowires and rods, demonstrated by few studies that have reported control over plasmon resonance properties.[24,25] Furthermore, for most preparation procedures, the problem of plasmon control is exacerbated by the rounding of facets[24] related to low selectivity between {110} and {100} facets upon surfactant binding.[26]

Herein we report the synthesis of pentagonal faceted silver rods with precise length and width control using decahedra[27] as well-defined intermediates and clearly identify the role of decahedra in the transformation mechanism. Plasmonic properties of the faceted rods and their SERS are described. Tunability of plasmonic properties of the rods and the versatility of the synthetic approach are demonstrated.

RESULTS AND DISCUSSION

Monodisperse decahedral AgNPs were prepared by photochemical synthesis described elsewhere.[27] The decahedra sizes could be controlled by regrowth from 30 to

See the accompanying Perspective by Skrabalak and Xia on p 10.

*Address correspondence to vkitaev@wlu.ca.

Received for review September 17, 2008 and accepted December 03, 2008.

Published online December 15, 2008.
10.1021/nn800591y CCC: $40.75

© 2009 American Chemical Society

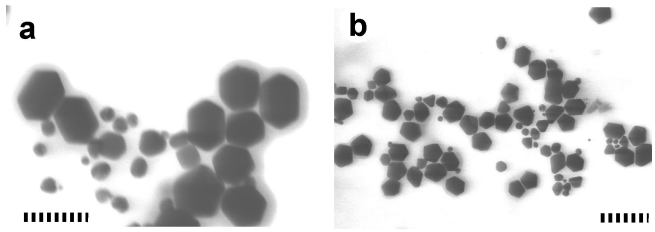

Figure 1. Representative TEM images of decahedra regrowth into faceted pentagonal rods performed in ethylene glycol at 150−180 °C. The scale bar is 100 nm for all images.

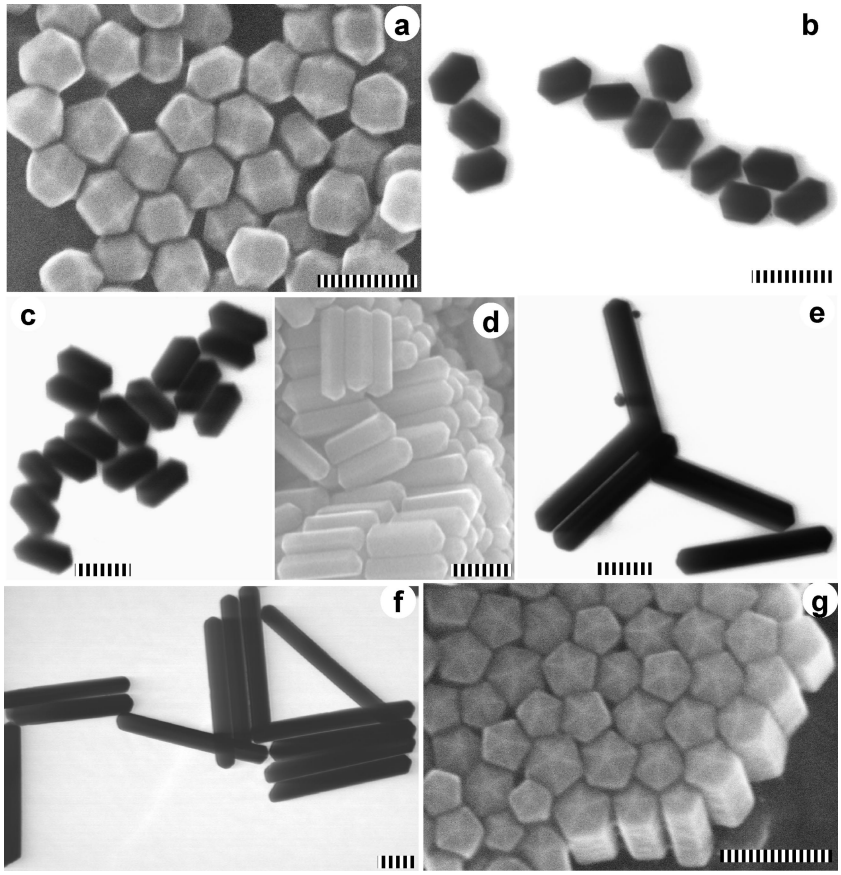

Figure 2. SEM and TEM images of faceted rod AgNPs prepared by the regrowth in aqueous solution. The rod length is (a) 62 ± 3 nm; (b) 75 ± 3 nm; (c) 108 ± 5 nm; (d) 142 ± 7 nm; (e) 260 ± 10 nm; (f) 430 ± 15 nm; (g) 138 ± 8 nm. The rod width is 49.5 ± 2.5 nm for (a)−(f) and 40 ± 5 nm for (g). The scale bar is 100 nm for all images.

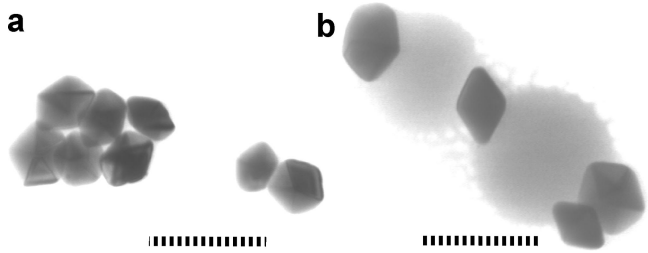

Figure 3. SEM images of the initial stages of the growth of pentagonal rods with (a) 40% and (b) 80% of new silver added relative to that present in the original decahedral AgNPs. The scale bar is 100 nm for all images.

120 nm and larger.[27] Since decahedra were postulated to be a key intermediate in the synthesis of silver and gold pentagonal rods,[12,30] different conditions of decahedra regrowth were explored after establishing their preparation. Initially, we were able to prove that decahedra conversion to rods is possible in a polyol process.[19,23] At the same time, even after considerable efforts, the rod yield could not be improved beyond *ca.* 30% (Figure 1). A likely reason for low yields in our regrowth attempts is that, at the synthesis temperature, added Ag^+ etches the decahedra surface faster compared to silver reduction by hot ethylene glycol.

Subsequently, thermal regrowth in water at 95 °C with citrate as a reducing (and stabilizing) agent was found to be optimal for high-yield rod preparation. Purified silver decahedra were introduced into a temperature-controlled solution immediately followed by silver nitrate addition. Polyvinylpyrrolidone (PVP) was found to improve the yield and stability of the resulting AgNPs, but not absolutely necessary for the shape transformation. The most notable aspect of the regrowth process is that it occurs exclusively one-dimensionally in the direction of the five-fold decahedra axis, as proposed in the literature.[12,30] This result was confirmed in several independent runs using identical seeds and regrowing them to rods with different aspect ratios. The resulting rod diameters within a margin of statistical error remained essentially the same as the diameter of the seed decahedral AgNPs. Such remarkable growth selectivity coupled with the full control over the rod length by varying the amount of silver added to decahedra seeds enables preparation of faceted pentagonal rods with desired length and thickness, shown in Figure 2.

To demonstrate precise control over pentagonal morphology, we judiciously created pentadecahedra (elongated pentagonal dipyramid, regular Johnson solid, J_{16}, also referred as Ino (truncated) decahedron for metal clusters[28]), which can be visualized as a decahedron stretched along the five-fold axis by square facets so that it retains a pentagonal cross section (Figures 2a and 6b). The J_{16} NP morphology has not been reported previously to the best of our knowledge. Additional evidence of length control during the decahedra regrowth is the ability to extend the decahedra by several nanometers demonstrated in Figure 3b.

The regrowth process is nearly flawless for rods with an aspect ratio (*L*/*D*) below 4 (Figure 2a−d). The rod yield progressively drops to 95% and below for *L*/*D* > 5. An *L*/*D* ratio of up to *ca.* 11 (Figures 2f and 4) can be readily achieved by semicontinuous silver addition.

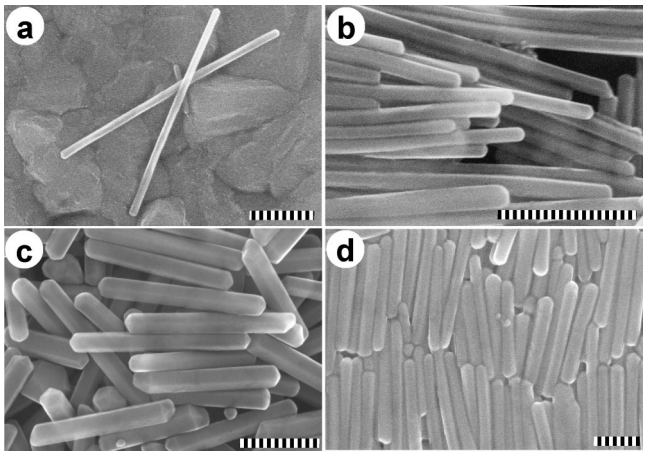

Figure 4. SEM images of longer pentagonal faceted rod AgNPs with the aspect ratios of (a) 8.7 and (b) 10.2; as well as (c) and (d) longer 2 μm pentagonal faceted rod AgNPs regrown in turn from *ca.* 0.5 μm rods. The scale bar is 100 nm for (a) and (b) and 2 μm for (c) and (d).

For further regrowth, quasi-spherical byproduct accumulates and purification becomes necessary. In an important development, we were able to restart regrowth of relatively long rods and obtain perfectly width-monodisperse and fairly length-monodisperse 2 μm rods (Figure 4c,d). Therefore, the reported regrowth process can be further optimized for synthesis of faceted rods with the length of several microns.

The visual changes accompanying rod growth are striking: first, the orange or red decahedra solution becomes yellow or yellow-orange as two plasmonic peaks merge at 430−440 nm (Figure 5) and the AgNPs become more isotropic as shown in Figure 2a,b. Upon further growth, the increase in elongation leads to a splitting of the plasmon peaks with the longitudinal peak shifting to longer wavelengths and into NIR. The sequence of color changes is represented in Figure 5a by photographs of solutions of the rods with different aspect ratios accompanied by the optical spectra in Figure 5b.

Noteworthy is the resolved doublet structure of the transverse plasmon (Figures 5b and 6a), which was predicted theoretically.[29] This doublet originates from two distinct surface plasmon modes supported by the pentagonal geometry. The resolved doublet highlights the uniformity and faceting of the pentagonal rod cross sections. With respect to faceting, there are two reasons that it is preserved in our preparation: (*i*) well-defined decahedra seeds and (*ii*) the absence of etching structure-directing agents, such as CTAB.[24,30] Exposing the synthesized faceted rods to CTAB or basic solutions with high pH > 11 resulted in rounding of their edges (Figure 7).

Another point worthy of mentioning is the rather uncommon ratio of intensities of the longitudinal and transverse plasmon peaks. This intensity of the longitudinal mode is typically significantly higher for most of the rods reported,[24,25] which is also supported by theoretical modeling. In this respect, it has to be realized that, in the case of pentagonal rods, there are two symmetric pencil-like tips. These tips effectively present a distribution of lengths that should broaden the longitu-

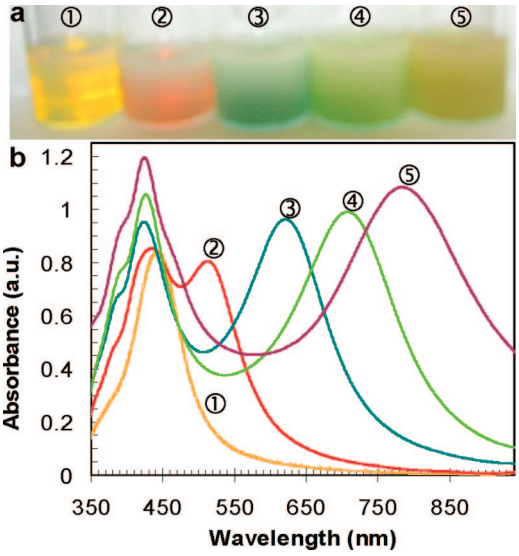

Figure 5. Optical properties of synthesized pentagonal faceted rod AgNPs. (a) Photographs of aqueous dispersions and (b) UV−vis spectra of pentagonal faceted rod AgNPs with the thickness of 49.5 ± 2.5 nm and length of (1) 62 ± 3 nm; (2) 75 ± 3 nm; (3) 108 ± 5 nm; (4)142 ± 7 nm; (5) 158 ± 8 nm.

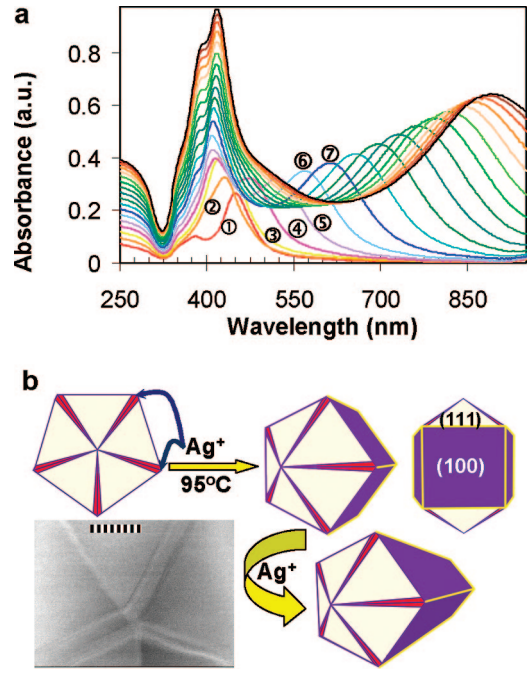

Figure 6. (a) UV−vis spectra of the growth kinetics of pentagonal faceted rod AgNPs monitored *in situ* at 95 °C for 17 min following silver addition. The final aspect ratio of the synthesized rods was *ca.* 2.7. Each curve is separated by 1 min interval. First four spectra in a sequence are labeled with circled symbols 1−4 for clarity. (b) Proposed mechanism for decahedra transformation to rods including HR-TEM evidence. The scale bar is 5 nm.

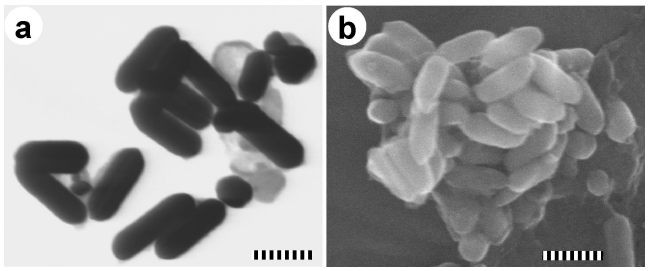

Figure 7. TEM and SEM images of rod AgNPs rounded by exposure to corrosive environment: (a) CTAB and (b) basic solutions with pH > 11. The scale bar is 100 nm for all images.

dinal plasmonic mode significantly. (Note that integrated intensity of the longitudinal mode is noticeably higher compared to the transverse one.) At the same time, metals rods reported and modeled so far had rounded or flat ends, which do not induce comparable broadening of the longitudinal plasmonic mode. It should be noted that the actual distribution of the length of the reported faceted rods is significantly better than the width distribution (*ca.* 5% *vs ca.* 10% standard deviation).

In accordance with the previously proposed models of silver anisotropic regrowth[31,32] and our evidence that the pentagonal cross section remains unchanged, the following transformation mechanism can be proposed (Figure 6b). Ag^+ is reduced by citrate (kinetically limiting stage), and silver deposition takes place in the areas of the highest surface energy in decahedra. Such areas are disclination wedges between facets arising from an intrinsic geometric misfit of five tetrahedral constituent units of a decahedron,[22] which are resolved in a HR-TEM image (Figure 6b). Following selective silver deposition into the wedges, {111} facets are continuously reconstructed with preserved dimensions, while new rectangular {100} facets[30] are progressively enlarged. Preferential stabilization of the pentagonal rim and {100} facets with citrate and PVP at higher temperatures[32,33] may be another contributing factor. The difference between thermal and photochemical decahedra regrowth is that the latter preserves the shape upon {111} facet enlargement[27] and likely initiates at the tips of the pentagonal rim, similarly to the silver prism growth *via* an active edge.[31] Supporting evidence for this scenario is the fact that decahedra overexposed to light in the absence of AgNP solution become partially truncated (rounded) at the vertices of the pentagonal rim.[27]

Due to excellent monodispersity and good stabilization in aqueous solution, our faceted pentagonal rod AgNPs readily self-assemble into densely packed rafts and arrays upon drying of their dispersions. Self-assembly is assisted by slower solvent evaporation (>5 min) and higher NP concentrations (2−5 mM silver). The self-assembled layers, shown in Figure 8, feature the structures similar to smectic mesophases. The order between the layers can be readily frustrated as shown in Figure 8b,d, while the regular arrangement within the layers is strongly persistent. Noteworthy, the long-range hexagonal order prevails within the layers despite the pentagonal symmetry of the rods (Figure 8c,e,f). This observation is consistent with the fact that five-fold symmetry is not compatible with the close packing that results from evaporation-induced self-assembly.[34] General trends of the self-assembly were explored upon variation of the *L*/*D* ratio. The self-assembly into well-defined layered structures starts to be observed for the pentagonal AgNPs with *L*/*D* ratio as low as 2. For the *L*/*D* > *ca.* 4, it seems that the silver nanorods do not have enough mobility in the dispersions to self-assemble readily into long-range structures, though the local ordering is typically observed. Figure 8d,f demonstrates more disordered packing for *L*/*D* = 3.7, our current boundary aspect ratio for the self-assembly. The best packing has been obtained for the particles with *L*/*D* about 2.5 (Figure 8a). Overall, re-

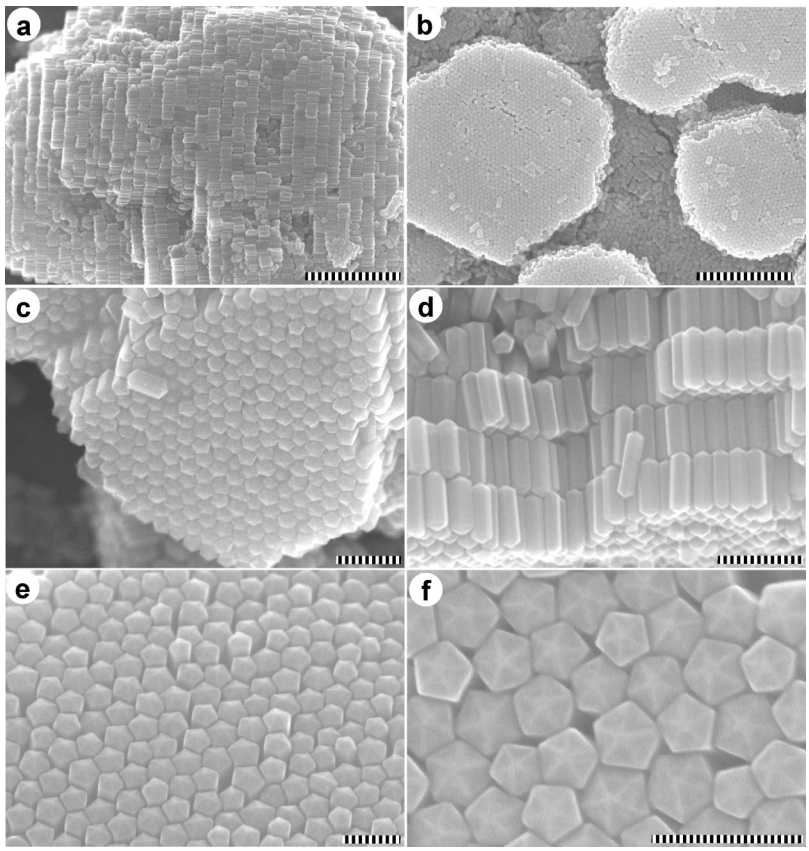

Figure 8. SEM images of self-assembled packing of monodisperse faceted pentagonal rod AgNPs. The rod length is 102 nm for (a) and (c), 123 nm for (b) and (e), and 142 nm for (d) and (f). The rod width is 38 nm for (c) and (f) and *ca.* 50 nm for the rest of the images. The scale bar is 1 μm for (a) and (b), 200 nm for (c) and (d), and 100 nm for (e) and (f).

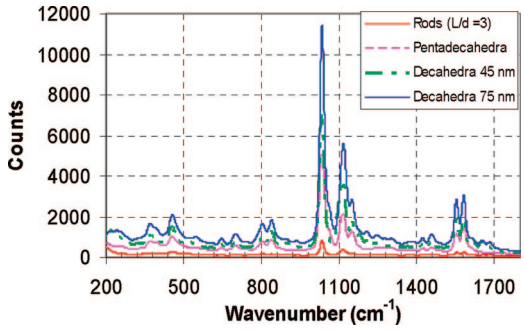

Figure 9. Comparison of surface-enhanced Raman scattering (SERS) efficiency of several decahedral and faceted rod AgNPs (with the same silver concentration and surface coverage of *ca.* 1.5 monolayers) using thiosalicylic acid as a probing molecule.

ported monodisperse nanoshapes provide ample opportunities to systematically explore packing arrangements of uniform nanoscale objects with five-fold symmetry.

Due to ease of preparation and excellent shape and size control, the reported faceted pentagonal rods should be attractive for most practical applications of metal NPs, such as in plasmonics,[5] sensing,[8] and medical treatment.[7] For instance, using Xia's approach to metal cages,[13] gold pentagonal shells with two plasmon absorption modes tunable across visible and NIR can be created. Pentagonal faceted AgNPs were also investigated for surface-enhanced Raman scattering (SERS) following the observation that decahedra SERS was superior to other common NP shapes, such as quasi-spherical particles and platelets.[27] Notably, rods showed less enhancement compared to decahedra of different sizes and the efficiency of SERS enhancement dropped with the increase in *L*/*D* (Figure 9). Supported also by the observation of minimal SERS enhancement in solution both for rods and decahedra, it suggests that interparticle cavities play a dominant role in this system.[35] The extensive interparticle spacing is typical for decahedra dry films[27] compared to more densely packed pentagonal rods (Figure 8).

In conclusion, decahedra regrowth into faceted pentagonal rods with the controlled dimensions has been reported, and the transformation pathway is elucidated. The rod length could be varied precisely during the regrowth, while the width was determined by the choice of decahedra seeds since rod growth occurs exclusively along the five-fold axis. High symmetry and low size variation of the synthesized silver nanoshapes resulted in narrow plasmon peaks tunable across the entire visible and NIR range. The faceted pentagonal rods self-assembled readily into highly ordered layered structures with the predominant hexagonal packing. In light of the reliable synthetic approach, high monodispersity, excellent size control, prominent optical properties, and propensity for self-assembly, the reported silver NPs should be attractive for diverse optical applications including plasmonics and photonic sensing.

METHODS

Reagents. Silver nitrate (99%), sodium citrate tribasic dihydrate (Aldrich 99+%), polyvinylpyrrolidone (PVP, M_w = 40K), sodium borohydride (99%), and L-arginine (TLC, 98%) were supplied by Aldrich and used as received. High-purity deionized water (>18.4 MΩ · cm) was produced using Millipore A10 Milli-Q.

Synthesis of Faceted Pentagonal Rod AgNPs. To prepare decahedral AgNPs, a precursor solution of silver NPs was first prepared using a mixture of 0.500 mL of 0.05 M sodium citrate, 0.015 mL of 0.05 M PVP, 0.050 mL of 0.005 M L-arginine, 0.200 mL of 0.005 M $AgNO_3$ and 7.0 mL of deionized water in a 20 mL vial reduced by 0.080 mL of 0.10 M $NaBH_4$. The resulting pale yellow solution was stirred until it became bright yellow after several minutes. The bright yellow solution was then exposed to a 400 W metal halide lamp (Sunmaster).[27] To produce smaller decahedra of 35−45 nm in a diameter largely used to prepare the rods, the blue light was used (LS-500-R-HS07 Corion filter) with the exposure time from 2 to 15 h depending on intensity.[27]

In the next step, 2.9 mL of the freshly prepared decahedral AgNP solution[27] was centrifuged to sediment particles and replace a supernatant with 1.0 mL of pure deionized water. The resulting silver concentration was *ca.* 0.33 mM. After supernatant replacement, the decahedral AgNPs should be used within a few days (while in presence of citrate and PVP, the decahedral AgNPs are stable for at least several months). Having prepared the decahedra seeds, 2.0 mL of water, 0.400 mL of 0.05 M sodium citrate, and 0.066 mL of 0.05 M PVP were heated to 95 °C in a 20 mL vial on a magnetic stirrer (Heidolph MR3004). After temperature equilibration, 1 mL of decahedra solution was added followed immediately by silver nitrate. Varying amounts of silver nitrate allowed producing rods of different length. Up to 0.15−0.20 mL of silver nitrate (0.005 M) can be added at once to produce rods with an aspect ratio up to 4−5 in high yield in 10−15 min of the reaction. To grow larger rods, 0.1 mL increments of $AgNO_3$ (0.005 M) were added every 10 min to produce rods with an aspect ratio up to 12. In a control experiment, rods with an aspect ratio of *ca.* 10 were centrifuged several times and their regrowth was restarted following the above procedure. The resulting rods reached the aspect ratio of *ca.* 40 (average length of 2 μm). Finally, adding 10 μL of 0.1 M KOH prior to decahedra and silver nitrate was found to improve the rod yield slightly but was not essential for the reaction.

Characterization. Electron microscopy (both TEM and SEM) was performed using Hitachi S-5200. Hitachi HD-2000 was used for HR-TEM. NP solutions were deposited on a carbon-coated Formvar grid (EMS Corp.). Operating voltage was 30.0 kV. The average size and standard deviation were determined from SEM and TEM images by averaging diameters of at least 100 particles. UV−vis spectra were acquired with either Ocean Optics QE65000 fiber-optic UV−vis spectrometer or Cary 50Bio UV−vis spectrophotometer. Raman spectra were recorded using R-3000QE fiber-optic Raman spectrometer equipped with 290 mW laser at 785 nm (RSI).

Acknowledgment. The authors gratefully acknowledge financial support by Natural Science and Engineering Research Council of Canada, Canada Foundation for Innovation, Ontario ORF-RI, Research Corporation (Cottrell Award), Wilfrid Laurier University and STEP. The Centre for Nanostructure Imaging (University of Toronto) is greatly appreciated for an access to Electron Microscopy facilities. The authors thank N. Coombs for HR-TEM decahedra imaging, S. Mamiche for technical assistance, and L. Cademartiri for valuable discussions.

REFERENCES AND NOTES

1. Sun, Y. G.; Xia, Y. N. Shape-Controlled Synthesis of Gold and Silver Nanoparticles. *Science* **2002**, *298*, 2176–2179.

2. Tao, A. R.; Habas, S.; Yang, P. Shape Control of Colloidal Metal Nanocrystals. *Small* **2008**, *4*, 310–325.
3. Pileni, M. P. Control of the Size and Shape of Inorganic Nanocrystals at Various Scales from Nano to Macrodomains. *J. Phys. Chem. C* **2007**, *111*, 9019–9038.
4. Burda, C.; Chen, X. B.; Narayanan, R.; El-Sayed, M. A. Chemistry and Properties of Nanocrystals of Different Shapes. *Chem. Rev.* **2005**, *105*, 1025–1102.
5. Lal, S.; Link, S.; Halas, N. J. Nano-Optics from Sensing to Waveguiding. *Nat. Photonics* **2007**, *1*, 641–648.
6. Liu, G. L.; Yin, Y.; Kunchakarra, S.; Mukherjee, B.; Gerion, D.; Jett, S. D.; Bear, D.; Gray, J. W.; Alivisatos, A. P.; Lee, L. P.; *et al.* A Nanoplasmonic Molecular Ruler for Measuring Nuclease Activity and DNA Footprinting. *Nat. Nanotechnol.* **2006**, *1*, 47–52.
7. Huang, X. H.; Jain, P.; El-Sayed, I. H.; El-Sayed, M. A. Gold Nanoparticles: Interesting Optical Properties and Recent Applications in Cancer Diagnostic and Therapy. *Nanomedicine* **2007**, *2*, 681–693.
8. Lu, W.; Lieber, C. M. Nanoelectronics from the Bottom Up. *Nat. Mater.* **2007**, *6*, 841–850.
9. Wiley, B. J.; Im, S. H.; Li, Z. Y.; McLellan, J.; Siekkinen, A.; Xia, Y. Maneuvering the Surface Plasmon Resonance of Silver Nanostructures through Shape-Controlled Synthesis. *J. Phys. Chem. B* **2006**, *110*, 15666–15675.
10. Dieringer, J. A.; McFarland, A. D.; Shah, N. C.; Stuart, D. A.; Whitney, A. V.; Yonzon, C. R.; Young, M. A.; Zhang, X. Y.; Van Duyne, R. P. Surface Enhanced Raman Spectroscopy: New Materials, Concepts, Characterization Tools, And Applications. *Faraday Discuss.* **2006**, *132*, 9–26.
11. Gu, G. H.; Kim, J.; Kim, L.; Suh, J. S. Optimum Length of Silver Nanorods for Fabrication of Hot Spots. *J. Phys. Chem. C* **2007**, *111*, 7906–7909.
12. Kneipp, K.; Kneipp, H.; Kneipp, J. Surface-Enhanced Raman Scattering in Local Optical Fields of Silver and Gold Nanoaggregatess—From Single-Molecule Raman Spectroscopy to Ultrasensitive Probing in Live Cells. *Acc. Chem. Res.* **2006**, *39*, 443–450.
13. Skrabalak, S. E.; Au, L.; Li, X. D.; Xia, Y. Facile Synthesis of Ag Nanocubes and Au Nanocages. *Nat. Protoc.* **2007**, *2*, 2182–2190.
14. Kim, F.; Connor, S.; Song, H.; Kuykendall, T.; Yang, P. D. Platonic Gold Nanocrystals. *Angew. Chem., Int. Ed.* **2004**, *43*, 3673–3677.
15. Sun, Y.; Gates, B.; Mayers, B.; Xia, Y. Crystalline Silver Nanowires by Soft Solution Processing. *Nano Lett.* **2002**, *2*, 165–168.
16. Wiley, B. J.; Xiong, Y. J.; Li, Z. Y.; Yin, Y. D.; Xia, Y. A. Right Bipyramids of Silver: A New Shape Derived from Single Twinned Seeds. *Nano Lett.* **2006**, *6*, 765–768.
17. Zhang, X.; Tsuji, M.; Lim, S.; Miyamae, N.; Nishio, M.; Hikino, S.; Umezu, M. Synthesis and Growth Mechanism of Pentagonal Bipyramid-Shaped Gold-Rich Au/Ag Alloy Nanoparticles. *Langmuir* **2007**, *23*, 6372–6376.
18. Wiley, B. J.; Chen, Y. C.; McLellan, J. M.; Xiong, Y. J.; Li, Z. Y.; Ginger, D.; Xia, Y. N. Synthesis and Optical Properties of Silver Nanobars and Nanorice. *Nano Lett.* **2007**, *7*, 1032–1036.
19. Wiley, B.; Sun, Y.; Xia, Y. Synthesis of Silver Nanostructures with Controlled Shapes and Properties. *Acc. Chem. Res.* **2007**, *40*, 1067–1076.
20. Hofmeister, H. Fivefold Twinned Nanoparticles. In *Encyclopedia of Nanoscience and Nanotechnology*; American Scientific: Stevenson Ranch, CA, 2004.
21. Jadzinsky, P. D.; Calero, G.; Ackerson, C. J.; Bushnell, D. A.; Kornberg, R. D. Structure of a Thiol Monolayer-Protected Gold Nanoparticle at 1.1 Angstrom Resolution. *Science* **2007**, *318*, 430–433.
22. Johnson, C. L.; Snoeck, E.; Ezcurdia, M.; Rodriguez-Gonzalez, B.; Pastoriza-Santos, I.; Liz-Marzan, L. M.; Hytch, M. J. Effects of Elastic Anisotropy on Strain Distributions in Decahedral Gold Nanoparticles. *Nat. Mater.* **2008**, *7*, 120–124.
23. Sun, Y.; Mayers, B.; Herricks, T.; Xia, Y. Polyol Synthesis of Uniform Silver Nanowires: A Plausible Growth Mechanism and the Supporting Evidence. *Nano Lett.* **2003**, *3*, 955–960.
24. Jana, N. R.; Gearheart, L.; Murphy, C. J. Wet Chemical Synthesis of Silver Nanorods and Nanowires of Controllable Aspect Ratio. *Chem. Commun.* **2001**, 617–618.
25. Orendorff, C. J.; Gearheart, L.; Jana, N. R.; Murphy, C. Aspect Ratio Dependence on Surface Enhanced Raman Scattering Using Silver and Gold Nanorod Substrates. *J. Phys. Chem. Chem. Phys.* **2006**, *8*, 165–170.
26. Wang, Z. L.; Mohamed, M. B.; Link, S.; El-Sayed, M. A. Crystallographic Facets and Shapes of Gold Nanorods of Different Aspect Ratios. *Surf. Sci.* **1999**, *440*, L809–L814.
27. Pietrobon, B.; Kitaev, V. Photochemical Synthesis of Monodisperse Size- Controlled Silver Decahedral Nanoparticles and Their Remarkable Optical Properties. *Chem. Mater.* **2008**, *20*, 5186–5190.
28. Cleveland, C. L.; Landman, U.; Schaaff, T. G.; Shafigullin, M. N.; Stephens, P. W.; Whetten, R. L. Growth and Form of Gold Nanorods Prepared by Seed-Mediated, Surfactant-Directed Synthesis. *Phys. Rev. Lett.* **1997**, *79*, 1873–1876.
29. Kottmann, J. P.; Martin, O. J. F. Plasmon Resonances of Silver Nanowires with a Nonregular Cross Section. *Phys. Rev. B* **2001**, *64*, 235402-1–235402-10.
30. Johnson, C. J.; Dujardin, E.; Davis, S. A.; Murphy, C. J.; Mann, S. Growth and Form of Gold Nanorods Prepared by Seed-Mediated, Surfactant-Directed Synthesis. *J. Mater. Chem.* **2002**, *12*, 1765–1770.
31. Lofton, C.; Sigmund, W. Mechanisms Controlling Crystal Habits of Gold and Silver Colloids. *Adv. Funct. Mater.* **2005**, *15*, 1197–1208.
32. Zhang, S. H.; Jiang, Z. Y.; Xie, Z. X.; Xu, X.; Huang, R. B.; Zheng, L. S. Growth of Silver Nanowires from Solutions: A Cyclic Penta-Twinned-Crystal Growth Mechanism. *J. Phys. Chem. B* **2005**, *109*, 9416–9421.
33. McEachran, M.; Kitaev, V. Direct Structural Transformation of Silver Platelets into Right Bipyramids and Twinned Cube Nanoparticles: Morphology Governed by Defects. *Chem. Commun.* **2008**, 5737–5739.
34. Dimitrov, A. S.; Nagayama, K. Continuous Convective Assembling of Fine Particles into Two-Dimensional Arrays on Solid Surfaces. *Langmuir* **1996**, *12*, 1303–1311.
35. Pieczonka, N.; Aroca, R. F. Single Molecule Analysis by Surfaced-Enhanced Raman Scattering. *Chem. Soc. Rev.* **2008**, *37*, 946–954.